The Evolution of Larger Size in High Altitude *Drosophila melanogaster* has a Polymorphic Genetic Architecture

Quentin D. Sprengelmeyer, Justin B. Lack, Dylan T. Braun, Matthew J. Monette, John E. Pool

Laboratory of Genetics, University of Wisconsin-Madison, Madison, WI, 53706

Running title: Polymorphic adaptation of size in flies

Keywords: Adaptive evolution, genetic architecture, size, Drosophila melanogaster, quantitative trait locus mapping, local adaptation, genetic differentiation

Corresponding author:
John E. Pool
425-G Henry Mall
Madison, WI 53706
+1-608-265-1036
jpool@wisc.edu

Abstract

Important uncertainties persist regarding the genetic architecture of adaptive trait evolution in natural populations, including the number of genetic variants involved, whether they are drawn from standing genetic variation, and whether directional selection drives them to complete fixation. Here, we take advantage of a unique natural population of *Drosophila melanogaster* from the Ethiopian highlands, which has evolved larger body size than any other known population of this species. We apply a bulk segregant quantitative trait locus (QTL) mapping approach to four unique crosses between highland Ethiopian and lowland Zambian populations for both thorax length and wing length. Results indicated a persistently variable genetic basis for these evolved traits (with largely distinct sets of QTLs for each cross), and at least a moderately polygenic architecture with relatively strong effects present. We complemented these mapping experiments with population genetic analyses of QTL regions and gene ontology enrichment analysis, generating strong hypotheses for specific genes and functional processes that may have contributed to these adaptive trait changes.

Finally, we find that the genetic architectures our QTL mapping results for size traits mirror those from similar experiments on other recently-evolved traits in this species. Collectively, these studies suggest a recurring pattern of polygenic adaptation in this species, in which causative variants do not approach fixation and moderately strong effect loci are present.

Introduction

Well into the genomic era, considerable debate persists over the types of genetic architectures that underlie adaptive evolution. For example, it is unclear how polygenic adaptive phenotypic changes tend to be – genes of major effect on adaptive traits are often reported (*e.g.* Miller et al. 2014; van't Hof et al. 2016), and in the case of local adaptation, these are more likely to overcome the homogenizing force of migration (Yeaman & Whitlock 2011). However, it is possible that most adaptive events may instead involve large numbers of small-effect changes (Pritchard & Di Rienzo 2010; Rockman 2011). It is also unclear how often adaptive variants are selected as newly occurring mutations (*e.g.* Linnen *et al.* 2009), versus selection on standing genetic variation after an environmental change (*e.g.* Colosimo *et al.* 2005). In the latter case, the detection of "soft sweeps" is a distinct and more challenging exercise than for classic "hard sweeps" (Pennings & Hermisson 2006). It is also unclear how often adaptive variants actually reach fixation, versus remaining polymorphic due to factors such as traits reaching a new optimum or threshold value, changes in selective pressures, balanced equilibria such as heterozygote advantage, or ongoing migration (Stephan 2016; Höllinger et al. 2019; Thornton 2019; Barghi & Schlötterer 2020; Barghi et al. 2020; Stephan & John 2020).

Population genomic scans for natural selection provide some insight into the genetic basis of adaptive evolution, identifying large numbers of loci with signals of recent positive selection, and estimating the frequency at which different functional categories of sites are targeted. However, the biological basis of natural selection at

66 these loci is usually not clear from genetic variation alone, and the properties of
67 adaptive mutations may depend on the biological process (*e.g.* morphological vs.
68 physiological changes; Carroll 2008; Liao et al. 2010). Therefore, an essential
69 complement to population genomic scans is detailed experimental case studies of
70 the genetic basis of specific adaptive phenotypic changes, in order to gain a clearer
71 and more nuanced understanding of how natural selection operates at the genetic
72 level.

73 The molecular and evolutionary genetics model *Drosophila melanogaster*
74 provides an efficient system for illuminating the genetic basis of evolutionary
75 change, in part because of its ease of laboratory study, its well-developed molecular
76 genetic toolkit, and its compact and well-annotated genome. *D. melanogaster*
77 expanded from a warm ancestral range in southern-central Africa to occupy diverse
78 worldwide environments (Sprengelmeyer et al. 2020). Latitude and especially
79 altitude gradients allow the comparison of geographically proximate, closely related
80 populations from contrasting environments. Phenotypic differences between
81 genetically similar populations provide ideal raw material for studies of evolution at
82 the genetic level, because the power of population genetic scans for local selection is
83 maximized, and once the relevant genes are identified, the number of plausible
84 causative mutations that differ between populations may be limited.

85 Size is a fundamental organismal quality. In *D. melanogaster* and other
86 Drosophilids, larger body size is correlated with cooler latitudes (David et al. 1977;
87 Gilchrist & Partridge 1999) and may provide a fitness advantage in cool
88 environments (McCabe & Partridge 1997; Reeve et al. 2000; Bochdanovits & De Jong

2003). Instead of a direct effect of size on thermal tolerance (*Drosophila* are small enough to be virtually isothermic with their environment), higher larval density in the tropics may select for earlier pupation, leading to smaller adults, while in cooler regions viability selection may favor larger, more robust adults (Partridge & French 1996).

In other Drosophilid species, larger flies are also found at higher altitudes (Stalker & Carson 1948; Norry et al. 2001), but this phenomonen was little studied in *D. melanogaster* until recently (Louis et al. 1982). In the past decade, a unique highland Ethiopian population of *D. melanogaster* was found to be the largest known naturally-occurring members of this species, with particularly enlarged wings (Pitchers et al. 2013; Klepsatel et al. 2013; Klepsatel et al. 2014; Fabian et al. 2015; Lack et al. 2016a; Lack et al. 2016b). The increase in wing size is associated with lower wing loading, which can improve flight performance (*e.g.* Petavy et al. 1997) and may benefit flies in highland environments that are persistently cool (limiting the speed of wing movement) and feature thinner air (providing less resistance against fly wings).

Comparing wing length between a highland Ethiopian population and a low altitude ancestral range population from Zabmia, phenotypic differentiation ($Q_{ST} =$ 0.985) greatly exceeded genetic differentiation (genome-wide $F_{ST} = 0.151$), implying that directional selection acted on wing length or a pleiotropically correlated trait (Lack et al. 2016a). The species is only estimated to have occupied the Ethiopian highlands about 2,700 years ago (Sprengelmeyer et al. 2020), or roughly 40,000 fly generations ago (based on 15 generations per year; Turelli &

Hoffmann 1995; Pool 2015). In light of an effective population size on the order of one million for this lineage (Sprengelmeyer et al. 2020), the evolution of larger size has occurred on a recent population genetic time scale (~0.01 autosomal coalescent units).

There has been some progress on understanding the tradeoffs and mechanisms involved in this population's size evolution. Compared to a low altitude Zambian population from the ancestral range, Ethiopian flies lay fewer but larger eggs, which develop into larger adults without prolonging the larval growth phase (Lack et al. 2016b). Ethiopian size changes were found to involve increases in cell size (likely a function of increased somatic ploidy; Smith and Orr-Weaver 1991; Edgar and Orr-Weaver 2001) as well as cell proliferation (Lack et al. 2016b). The evolution of larger wings in Ethiopian *D. melanogaster* was accompanied by a decanalization of wing development, implying that ancestral buffering mechanisms had been disrupted in the course of adaptive trait evolution (Lack et al. 2016a).

The genetic basis of Ethiopian size evolution has not been investigated. Outside Africa, initial progress has been made to identify genes underlying latitude-size clines in *D. melanogaster* outside Africa. In Australia, *Dca* and *srp* are potential contributors to wing and body size differences, respectively (Lee et al. 2011; Chen et al. 2012). Association testing (Jumbo-Lucioni et al. 2010) and experimental evolution (Turner et al. 2011) have suggested that many genes could influence within-population body size variation. However, quantitative trait locus (QTL) mapping of size differences between high and low latitude populations has suggested a few major loci, with uneven chromosomal contributions not predicted

by a highly polygenic model (Calboli et al. 2003). Hence, the polygenicity of body size variation may depend on whether diversity is examined within populations where stabilizing selection may predominate, or between populations where adaptive phenotypic evolution is suspected.

In this study we aim to understand the genetic architecture of adaptive trait evolution, using the Ethiopian population's thorax and wing size changes as model traits. Here, thorax legnth represents a proxy for overall body size, whereas wing length represents a trait that has particularly evolved in this population. We focus on the polygenicity of trait evolution and genetic predictability within a population. We perform bulk segregant analysis to ascertain QTLs that are involved in thorax and wing size trait evolution. We also use population genetic statistics and Gene Ontology enrichment to find evidence of local adaptation and to identify candidate genes for future functional investigation.

Material and Methods

Experimental Populations

All flies used in the experiment had been inbred for 8 generations from wild-caught isofemale lines (Lack et al. 2015). The populations came from Fiche, Ethiopia (EF, 9.81° N, 38.63° E, alt. 3070 m) and Siavonga, Zambia (ZI, 16.54° S, 28.72° E, alt. 530 m). These strains were free of any common polymorphic inversions. All flies used were raised at 20° C on medium prepared in batches of 4.5 L water, 500 mL cornmeal, 500 mL molasses, 200 mL yeast, 54 g agar, 20 mL propionic acid, and 45 mL tegosept 10% (in 95% ethanol).

158

159 *Bulk Segregant Analysis*

160 To determine what region of the genome harbor the causative variants
161 responsible for the evolution of larger thorax and wing size, bulk segregant analysis
162 was performed to detect quantitative trait loci (QTL). Four different population
163 cages were started with unique strains of smaller thorax and wing size (Zambia)
164 and thorax and wing population (Ethiopia) lines. Each population cage is 28 x 14 x
165 15 cm and has 14 vials containing the above medium. In each population cage,
166 reciprocal crosses were established between eight inbred parental individuals of
167 each strain (Zambia and Ethiopia). From each reciprocal cross, 125 F1 offspring of
168 each sex were used to establish the second generation. For the duration of the
169 experiment, non-overlapping generations were maintained at ~1200 individuals
170 (Figure 1). Adult flies were allowed to lay eggs on the food for one week before
171 being removed. The food vials were replaced when adult flies in the cage were 7-10
172 days old. At the 16th generation, 600 3-5 day old female flies from each population
173 cage were measured as described below. For each trait, thorax size and wing size,
174 the flies were placed into pools constituting the 10% smallest (N=60) and 10%
175 largest (N=60) individuals, with the remaining individuals discarded.

176

177 *Body Size*

178 To measure thorax and wing size, we followed the protocol described in Lack
179 et al. (2016a). Thorax size measurements were in 3-5 day old adult females. From
180 each mapping cross, females were photographed with a digital camera attached to a

stereo dissecting microscope (AmScope SM-4BX), and thorax length was measured from the base of the anterior humeral bristle to the posterior tip of the scutellum (Lack et al. 2016a). For wing size, we also examined 3-5 day old adult females from each of the mapping crosses. For five females per cross, a wing was removed and photographed at 509 magnification using a digital camera attached to a compound microscope (Olympus BH-2). The length and depth of each wing were then measured using ImageJ version 1.48 (http://imagej.nih.gov/ij/), we measured a straight line drawn from the intersection of the anterior crossvein and L4 longitudinal vein, to where the L3 longitudinal vein intersects the wing margin. For depth, we measured a straight line from the intersection of the L5 longitudinal vein and the posterior wing margin, passing through the intersection of the posterior crossvein and L4, and terminating at the anterior wing margin. For wing area, we imaged individual wings using the "wing grabber" apparatus described by Houle et al. (2003), and wing area was determined by outlining each wing using ImageJ version 1.48 (http://imagej.nih.gov/ij/), and the reported area for each cross is the mean of the five wings.

Genome preparation

We sequenced the genomes of pooled samples (N=30 individuals) for the parental lines and two such pools for each of the large- and small-size groups (0-5% and 5-10% extremes for each direction, summing to N=60 total for each extreme). Genomic DNA was obtained using a chloroform extraction and ethanol precipitation protocol. The DNA was fragmented with a Bioruptor sonicator (Diagenode), and

204 paired-end libraries with ~300 bp inserts prepared using NEBNext DNA Library
205 Prep Reagent Set for Illumina (New England Biolabs no. E6000L). Each library's
206 concentration and quality was analysed with an Agilent 2100 Bioanalyzer (Agilent
207 Technologies, Inc.). The prepared libraries were sequenced at UW-Madison
208 Biotechnology Center on the Illumina HiSeq 2000 platform. Having concluded that
209 the full 10% extremes would best be analyzed together (Pool 2016), we merged
210 reads from the 0-5% and 5-10% pools (similar numbers of reads were obtained
211 from these pools in each case) before proceeding with the analysis.
212
213 *Genome alignment*

214 All the raw data that passed the Illumina filters were processed using a Perl-
215 scripted pipeline. Reads from each sequenced genome were mapped to the *D.*
216 *melanogaster* reference genome (release 5.57) obtained from Flybase
217 (www.flybase.org), with the default parameters in BWA ver. 0.6.2-r126 (Li and
218 Durbin 2009). Using Stampy ver. 1.0.21(Lunter and Goodson 2011), the BAM files
219 were then remapped. With samtools ver. 0.1.18 (Li et al. 2009) reads were filtered
220 for a mapping quality of 20 and for proper pairs. The BAM files were further
221 processed by removing unmapped reads and sorted by coordinate, and PCR
222 duplicates were marked using Picard ver. 1.109 (http://picard.sourceforge.net). To
223 improve the alignment around indels we used GATK ver. 3.2 (McKenna et al. 2010).
224 The average depth of coverage per genome was calculated for the parental lines and
225 the low and high tolerant lines (Table S1).

226

227 *Quantitative Trait Locus (QTL) Mapping*

228 Synchronised mpileup files for the aligned genomes were created with the
229 PoPoolation2 ver. 1.201 software package (Kofler et al. 2011). The two large (and
230 two small) pools from a given cross were then combined with a custom perl script.
231 Ancestry difference (a_d) was then calculated with each biallelic SNP (Bastide et al.
232 2016). Ancestry difference estimates the difference between the proportion of the
233 large-fly pool's sequencing reads carrying an allele from the large (Ethiopia)
234 parental line and that same proportion from the small-fly pool. It was estimated as:

235 $$\textit{Equation 1: } a_d = (f_L - f_S) \,/\, (p_L - p_S)$$

236 Where p_L is the frequency of the major allele in the large parent, p_S is the small
237 parental allele, f_L is the frequency of the large parent allele in the large pool of F16
238 offspring, and f_S is that same allele's frequency in small F16 offspring. The five
239 chromosomal arms (X, 2L, 2R, 3L, and 3R) were divided into windows based on SNP
240 density (Lack et al. 2015) which created 2728, 3131, 2357, 2956, and 2935
241 windows respectively, each roughly 8.4-kb in size on average. Only sites that had a
242 parental strain frequency difference of ≥ 0.25 were used in the analysis. A
243 simulation-based inference for BSA mapping (SIBSAM) was performed (Pool 2016)
244 to identify significant QTLs and calculate their confidence intervals and effect sizes.
245 The scripts used for SIBSAM can be found at:
246 http://github.com/JohnEPool/SIBSAM1. SIBSAM is able to evaluate both primary
247 QTL peaks and flanking secondary QTL peaks, evaluating whether ragged peaks

248 contain significant evidence for more than one QTL. Forward simulations
249 incorporate recombination in multiple individuals for multiple generations,
250 selection on phenotype in the final generation with additivity, plus environmental
251 variance, and then the sampling of sequence reads to obtain a_d.
252
253 *Genetic differentiation and Gene Ontology (GO) enrichment analysis*
254 QTLs identified in the previous step will contain many genes that may or may
255 not be involved in the evolution of these traits. To help identify the causative genes
256 within the significant QTLs for thorax and wing size, window F_{ST} and maximum SNP
257 F_{ST} per window ("SNP F_{ST}"), and the haplotype statistic χ_{MD} (Lange & Pool 2016)
258 were analyzed. Genomes from Zambia (n=197) and Ethiopia (n=68) were used
259 from the *Drosophila* Genome Nexus (Lack et al. 2015). The χ_{MD} compares length of
260 identical haplotype blocks among individuals in one population versus another. The
261 comparisons are made within each of the five chromosomal arms (X, 2L, 2R, 3L, and
262 3R), which were divided into windows based on SNP density (Lack et al. 2015)
263 which created 2728, 3131, 2357, 2956, and 2935 windows respectively each
264 roughly 8.4-kb in size on average. To narrow down potential candidate genes, a
265 chromosomal arm quantile outlier approach was used to identify genes with an
266 extreme population genetic signal. We classified outlier regions windows that were
267 in the top 2.5% quantile in any of the three statistics. In order to form an outlier
268 region, a maximum of two non-outlier windows are allowed between two outlier
269 windows. Genes associated with outlier windows (overlapping them or the nearest
270 gene in either direction) were retained for subsequent analysis.

We preformed a gene ontology (GO) enrichment analysis to identify potential functional categories that may contribute to the contrasting phenotypes found between the Zambia and Ethiopia populations. The outlier genes that were identified in the significant QTL regions were used for window-based GO enrichment analysis (Pool et al. 2012). A GO enrichment analysis was conducted for both thorax and wing size. A *P* value was calculated based on the probability of observing a given number of outlier genes from a GO category. *P* values were obtained from permutation in which outlier regions were randomly reassigned 10,000 times.

Results

Quantitative Trait Locus (QTL) Mapping

We used bulk segergant analysis to perform QTL mapping for both thorax and wing length using 4 different unique between-population crosses. Each mapping population used individual inbred strains from an ancestral range Zambia population smaller thorax and wing length, and from the high altitude Ethiopia population that has evolved larger thorax and wing length. In our bulk segergant analysis, offspring of reciprocal crosses were allowed to interbreed for 16 non-overlapping generations without selection at a large population size ($N \approx 1{,}200$). After the 16^{th} generation, 600 adult females were measured for both thorax and wing length and the top and bottom 10% of individuals were grouped for pooled genomic sequencing (Figure 1; Materials and Methods). SIBSAM (Pool 2016) was

293 then used to identify primary and secondary QTL peaks, along with their estimated
294 effect sizes and genomic confidence intervals.
295
296 *QTL mapping*
297 For thorax length, four Ethiopia × Zambia mapping crosses revealed a total
298 of 12 significant peaks (Figure 2; Table S2). The EF8N cross had one significant peak
299 with an estimated effect size of ~17%. EF15N had two significant peaks, each having
300 an estimated effect size of ~15%. EF73N had the most significant peaks with a total
301 of five, and these had estimated effect sizes that ranged between 12% and 20%.
302 EF86N had four significant peaks with estimated effect sizes between 13% and 16%.
303 For wing length, these same four crosses revealed a total of 33 significant
304 peaks (Figure 3; Table S3). EF8N had a total of twelve significant peaks, with
305 estimated effect sizes that ranged between 7% and 24%. EF15N had 3 significant
306 peaks, with estimated effect sizes that range between 16% and 24%. EF73N had a
307 total of 10 significant peaks, with estimated effect sizes that ranged between 6% and
308 27%. EF86N had 8 significant peaks, with estimated effect sizes that ranged
309 between ~11%-25%.
310 In general, very different QTL landscapes were observed between
311 independent Ethiopia/Zambia crosses (Figure 3). In some cases, QTLs do overlap
312 between crosses, which may reflect either chance (different QTLs located close
313 together) or else genuine sharing of causative variants underlying thorax and/or
314 wing size. We identified QTL overlap when the QTL peak of one cross overlaps with
315 the genomic confidence interval of another cross. For thorax length there are no

316 regions between the four Ethiopia crosses where a QTL peak overlapped with
317 another peak's genomic confidence interval (Figure 4). However, for wing length
318 between the four crosses there were 12 regions where QTL peaks overlapped with
319 genomic confidence intervals involving 12 of the 33 QTLs (Figure 4). Within these
320 overlapping peaks there are no overlap between all four crosses.

321 Some differences in the significant QTLs between crosses could represent
322 chance detection of a shared QTL in some crosses but not others. However, with this
323 experimental design we expect to have >90% power to detect a QTL with 20%
324 effect size (Pool 2016). Hence, at least for several of the strongest of the QTLs
325 detected here, their absence in other crosses is likely to reflect real differences in
326 genetic architecture.

327

328 *Potential Targets of Local Adaptation Within QTL Regions*

329 Regions of the genome where the Zambia and Ethiopia populations greatly
330 differ in their genetic variation may harbor genes involved in these adaptive traits.
331 We used three population genetic statistics, window F_{ST}, maximum SNP F_{ST} within a
332 window, and the haplotype statistic χ_{MD} to identify possible candidate genes for
333 body and wing size evolution within the significant QTLs. Using three different
334 statistics is advantageous due to the differing power each statistic has in detecting
335 local adaptation, depending on whether selective sweeps are complete or
336 incomplete, or hard versus soft (Lange & Pool 2016). A quantile approach was used
337 identify only regions that had one of the three statistics with a quantile below 0.025
338 (Tables S4 & S5). There are many genes within these outlier regions with no known

role in either thorax or wing size. However, there are also genes known to be involved in size regulation.

For thorax length, genes corresponding to QTLs and population genetic outliers that are known to be involved in growth included *ct* (Thumm & Kadowaki 2001), *spi* (Nagaraj et al. 1999), *bbc* (Liu et al. 2014), *msn* (Kadrmas et al. 2004), *RasGAP1* (Dworkin & Gibson 2006), *scyl* (Reiling and Hafen 2004), and *tara* (Bejarano et al., 2008). Of these, *bbc* and *RasGAP1* provide examples of loci with promisingly narrow F_{ST} peaks at the SNP level (Figure 5), which may merit targeted investigation by future studies. We noted that *RasGAP1* is also within a wing QTL, and is therefore relevant to the analysis described below as well.

Within the outlier regions for wing length, these genes included *Dronc* (Verghese et al. 2012), *Dlish* (Wang et al. 2019), *fj* (Villano & Katz 1995), *Pka-C3* (Dworkin & Gibson 2006), *salr* (Wang et al.2017), and *Gbp1* (Koyama and Mirth 2016). *Dlish* and *Pka-C3* are examples of genes with individual SNPs having high F_{ST} values (Figure 6). Further functional testing will need to be conducted to establish if genetic variants found within these genes are indeed responsible for the associated phenotypes.

Gene Ontology (GO) Enrichment

We conducted individual GO enrichment analysis for thorax and wing length. We used only the genes found in the outlier windows located within significant QTL regions from the four crosses. Functional categories that yielded raw *P* values below 0.001 are listed in Tables S6 & S7. These included categories either known or

potentially involved in body and wing size. For thorax size, the top categories included: negative regulation of Ras protein signal transduction (Prober & Edgar 2002), regulation of protein polymerization (Fernández et al. 2011), and brahma complex (Krupp et al. 2005). For wing size, the top categories included: neurogenesis (Rutledge et al. 1992), ubiquitin protein ligase binding (Cornell et al. 1999), cellular amino acid catabolic process (Zinke et al. 1999), cellular response to anoxia (Heinrich et al 2011), transmembrane transport (Bartscherer et al. 2006), and negative regulation of proteolysis (Lee et al. 2001). Some of these functional processes might underlie Ethiopia size adaptation, while others may be driven by unrelated trait evolution in this high altitude population.

Discussion

We employed quantitive and population genetic strategies to investigate the genetic architecture of adaptive size evolution in our highland Ethiopia population. Our bulk segergant analysis revealed that between the four crosses, thorax size has 12 associated QTLs with moderate to large effect (~13-20%). However, between the four crosses wing size has 33 QTLs with small to large effects QTLs (~6-27%). A greater ability to detect wing length QTLs than thorax length QTLs may reflect the greater magnitude of the population difference in this trait (Lack et al. 2016b).

One striking result was the lack of QTL overlap between crosses for either thorax or wing size. Between the four thorax crosses there is no overlap. This is especially notable given that we have almost have very high power to detect QTLs with effect size of 20% (Pool 2016) and yet the QTL on chromosome arm 2L with

385 ~20% effect size is not present in any other cross. For wing size, there was overlap
386 in only 12 of the 33 QTL regions and no overlap between all four crosses. The QTLs
387 with the three largest effect sizes of over 25% are present in only one cross. The low
388 QTL overlap between crosses could reflect persistent genetic variation at cauasative
389 loci in the Ethiopian and/or Zambian populations. Given that the Ethiopian
390 population appears to have experienced directional selection for larger size, and still
391 maintains similar genetic variance for size traits as Zambia (Lack et al. 2016b), we
392 suggest that some favored size variants have not reached fixation in the Ethiopian
393 population. There are multiple reasons why favored alleles might not fix, including
394 the Ethiopian population reaching its new optimum or threshold trait value
395 (especially if ample standing variation means that not all large alleles needed to fix),
396 heterozygote advantage, or ongoing adaptation. Indeed, simulation and theory have
397 shown that depending on the genetic architecture of an adaptive trait, non-fixed
398 causative variants may be the norm (Stephan 2016; Höllinger et al. 2019; Thornton
399 2019; Barghi & Schlötterer 2020; Barghi et al. 2020; Stephan & John 2020).
400 Our conclusions of persistent variability underlying an evolved trait mirror
401 similar results for pigmentation (Bastide et al. 2016) and for ethanol resistance
402 (Sprengelmeyer et al. 2021) in this same population and others, all from mapping
403 experiments with similar design and scale. With five traits now examined (ethanol
404 resistance, abdominal background color, abdominal stripe width, thorax length, and
405 wing length), consistent patterns are starting to emerge. First, these traits each
406 average at least a few detectable QTLs per cross, with means ranging from 3 to 8.25
407 (Table 1). Second, there is notably little QTL peak overlap between parallel mapping

crosses involving different strains from the same populations. Wing length and ethanol resistance have the most overlap between crosses with ~35% (Table. 1). However, thorax size crosses do not have any overlap. For each of these traits, there are moderately large effect QTLs not present in other crosses. Hence, at the population level, it is fair to say that each of these traits is at least moderately polygenic, and involves non-fixed differences between populations. Third, moderately strong QTLs are consistently present in any given cross, with the average QTL effect size ranging from 13-19% (Table 1), although undetectable smaller effects may be present as well.

Polygenic adaptation may have diverse outcomes, depending in part on the number of segregating variants at the onset of selection that affect a trait, as well as the magnitudes of their effect on the trait relative to the shift in trait optimum. While each of the traits summarized above might be described as "polygenic", it is worth considering the type of polygenic adaptation that these mapping studies imply. The persistently variable genetic basis of these evolved traits may suggest a scenario of abundant standing genetic variation prior to selection for each of these traits. In light of the consistent presence of moderately strong QTLs for these traits, such standing variation may have included relatively large effect loci, which would experience relatively stronger directional selection during the trait's evolution. An abundance of standing variation is consistent with the large population size and high genetic diversity of this species (*e.g.* Sprengelmeyer et al. 2020). Further studies will be needed to quantify the models of polygenic adaptation that experiments such as ours indicate, and to assess whether such persistent variability

is a widespread outcome of trait evolution not only in this species but across the tree of life.

Acknowledgments

We would like to thank Jeremy Lange and Tiago Ribeiro for their help with bioinformatics and data collection in this project. We also thank the UW-Madison Center for High Throughput Computing (CHTC) for computational resources and assistance. This research was was supported by the National Institutes of Health grants R01 GM111797, R01 GM127480, R35 GM136306, F32 GM106594, and T32 GM007133.

Data Availability

All raw sequence data has been deposited in the NIH Short Read Archive, with accession numbers given in Table S1.

Literature Cited

Barghi, N., Hermisson, J., & Schlötterer, C. (2020). Polygenic adaptation: A unifying framework to understand positive selection. *Nature Reviews Genetics*, *21*(12), 769–781.

Bartscherer, K., Pelte, N., Ingelfinger, D., & Boutros, M. (2006). Secretion of Wnt Ligands Requires Evi, a Conserved Transmembrane Protein. *Cell*, *125*(3), 523–533.

Bastide, H., Yassin, A., Johanning, E. J., & Pool, J. E. (2014). Pigmentation in *Drosophila melanogaster* reaches its maximum in Ethiopia and correlates most strongly with ultra-violet radiation in sub-Saharan Africa. *BMC Evolutionary Biology*, *14*, 179.

460 Bastide, H., Lange, J. D., Lack, J. B., Yassin, A., & Pool, J. E. (2016). A variable genetic
461 architecture of melanic evolution in *Drosophila melanogaster*. *Genetics*, *204*(3),
462 1307-1319.
463
464 Bejarano, F., Luque, C. M., Herranz, H., Sorrosal, G., Rafel, N., Pham, T. T., & Milán, M.
465 (2008). A Gain-of-Function Suppressor Screen for Genes Involved in Dorsal–Ventral
466 Boundary Formation in the *Drosophila* Wing. *Genetics*, *178*(1), 307–323.
467
468 Bochdanovits, Z., & De Jong, G. (2003). Temperature dependence of fitness
469 components in geographical populations of *Drosophila melanogaster*: changing the
470 association between size and fitness. *Biological Journal of the Linnean Society*,
471 80(4), 717-725
472
473 Calboli, F. C. F., Kennington, W. J., & Partridge, L. (2003). Qtl Mapping Reveals a
474 Striking Coincidence in the Positions of Genomic Regions Associated with Adaptive
475 Variation in Body Size in Parallel Clines of *Drosophila melanogaster* on Different
476 Continents. *Evolution*, *57*(11), 2653–2658.
477
478 Carroll, S. B. (2008). Evo-Devo and an Expanding Evolutionary Synthesis: A Genetic
479 Theory of Morphological Evolution. *Cell*, *134*(1), 25–36.
480
481 Chen, Y., Lee, S. F., Blanc, E., Reuter, C., Wertheim, B., Martinez-Diaz, P., Hoffmann, A.
482 A., & Partridge, L. (2012). Genome-Wide Transcription Analysis of Clinal Genetic
483 Variation in *Drosophila*. *PLOS ONE*, *7*(4), e34620.
484
485 Colosimo, P. F., Hosemann, K. E., Balabhadra, S., Villarreal, G., Dickson, M., Grimwood,
486 J., Schmutz, J., Myers, R. M., Schluter, D., & Kingsley, D. M. (2005). Widespread
487 Parallel Evolution in Sticklebacks by Repeated Fixation of Ectodysplasin Alleles.
488 *Science*, *307*(5717), 1928–1933.
489
490 Cornell, M., Evans, D. a. P., Mann, R., Fostier, M., Flasza, M., Monthatong, M.,
491 Artavanis-Tsakonas, S., & Baron, M. (1999). The Drosophila melanogaster
492 Suppressor of deltex Gene, a Regulator of the Notch Receptor Signaling Pathway, Is
493 an E3 Class Ubiquitin Ligase. *Genetics*, *152*(2), 567–576.
494
495 David, J. R., Bocquet, C., & De Scheemaeker-Louis, M. (1977). Genetic latitudinal
496 adaptation of *Drosophila melanogaster*: new discriminative biometrical traits
497 between European and equatorial African populations. *Genet. Res.*, 30, 247-255.
498
499 de Jong, G., & Bochdanovits, Z. (2003). Latitudinal clines inDrosophila melanogaster:
500 Body size, allozyme frequencies, inversion frequencies, and the insulin-signalling
501 pathway. *Journal of Genetics*, *82*(3), 207–223.
502
503 Dworkin, I., & Gibson, G. (2006). Epidermal Growth Factor Receptor and
504 Transforming Growth Factor-β Signaling Contributes to Variation for Wing Shape in
505 *Drosophila melanogaster*. *Genetics*, *173*(3), 1417–1431.

Edgar, B. A., & Orr-Weaver, T. L. (2001). Endoreplication Cell Cycles: More for Less. *Cell*, *105*(3), 297–306.

Fabian, D. K., Lack, J. B., Mathur, V., Schlötterer, C., Schmidt, P. S., Pool, J. E., & Flatt, T. (2015). Spatially varying selection shapes life history clines among populations of *Drosophila melanogaster* from sub-Saharan Africa. *Journal of Evolutionary Biology*, *28*(4), 826–840.

Fernández, B. G., Gaspar, P., Brás-Pereira, C., Jezowska, B., Rebelo, S. R., & Janody, F. (2011). Actin-Capping Protein and the Hippo pathway regulate F-actin and tissue growth in *Drosophila*. *Development*, *138*(11), 2337–2346.

Gilchrist, A. Stuart, & Partridge, L. (1999). A Comparison of the Genetic Basis of Wing Size Divergence in Three Parallel Body Size Clines of *Drosophila melanogaster*. *Genetics*, *153*(4), 1775–1787.

Heinrich, E. C., Farzin, M., Klok, C. J., & Harrison, J. F. (2011). The effect of developmental stage on the sensitivity of cell and body size to hypoxia in *Drosophila melanogaster*. *Journal of Experimental Biology*, *214*(9), 1419–1427.

Hermisson, J., & Pennings, P. S. (2005). Soft Sweeps: Molecular Population Genetics of Adaptation From Standing Genetic Variation. *Genetics*, *169*(4), 2335–2352.

James, A. C., Azevedo, R. B., & Partridge, L. (1995). Cellular basis and developmental timing in a size cline of *Drosophila melanogaster*. *Genetics*, *140*(2), 659–666.

Höllinger, I., Pennings, P. S., & Hermisson, J. (2019). Polygenic adaptation: From sweeps to subtle frequency shifts. *PLOS Genetics*, *15*(3), e1008035.

John, S., & Stephan, W. (2020). Important role of genetic drift in rapid polygenic adaptation. *Ecology and Evolution*, *10*(3), 1278–1287.

Jumbo-Lucioni, P., Ayroles, J. F., Chambers, M. M., Jordan, K. W., Leips, J., Mackay, T. F., & De Luca, M. (2010). Systems genetics analysis of body weight and energy metabolism traits in *Drosophila melanogaster*. *BMC Genomics*, *11*(1), 297.

Kadrmas, J. L., Smith, M. A., Clark, K. A., Pronovost, S. M., Muster, N., Yates, J. R., III, & Beckerle, M. C. (2004). The integrin effector PINCH regulates JNK activity and epithelial migration in concert with Ras suppressor 1. *Journal of Cell Biology*, *167*(6), 1019–1024.

Klepsatel, P., Gáliková, M., Maio, N. D., Huber, C. D., Schlötterer, C., & Flatt, T. (2013). Variation in Thermal Performance and Reaction Norms Among Populations of *Drosophila melanogaster*. *Evolution*, *67*(12), 3573–3587.

552 Klepsatel, P., Gáliková, M., Huber, C. D., & Flatt, T. (2014). Similarities and
553 Differences in Altitudinal Versus Latitudinal Variation for Morphological Traits in
554 *Drosophila melanogaster*. *Evolution*, *68*(5), 1385–1398.
555
556
557 Kofler, R., Pandey, R. V., & Schlötterer, C. (2011). PoPoolation2: identifying
558 differentiation between populations using sequencing of pooled DNA samples (Pool-
559 Seq). *Bioinformatics*, *27*(24), 3435-3436.
560
561 Koyama, T., & Mirth, C. K. (2016). Growth-Blocking Peptides As Nutrition-Sensitive
562 Signals for Insulin Secretion and Body Size Regulation. *PLOS Biology*, *14*(2),
563 e1002392.
564
565 Krupp, J. J., Yaich, L. E., Wessells, R. J., & Bodmer, R. (2005). Identification of Genetic
566 Loci That Interact With cut During Drosophila Wing-Margin Development. *Genetics*,
567 *170*(4), 1775–1795.
568
569 Lack, J. B., Cardeno, C. M., Crepeau, M. W., Taylor, W., Corbett-Detig, R. B., Stevens, K.
570 A., Langley, C. H., & Pool, J. E. (2015). The Drosophila genome nexus: a population
571 genomic resource of 623 *Drosophila melanogaster* genomes, including 197 from a
572 single ancestral range population. *Genetics*, *199*(4), 1229-1241.
573
574 Lack, J. B., Monette, M. J., Johanning, E. J., Sprengelmeyer, Q. D., & Pool, J. E. (2016a).
575 Decanalization of wing development accompanied the evolution of large wings in
576 high-altitude *Drosophila*. *Proceedings of the National Academy of Sciences*, *113*(4),
577 1014-1019
578
579 Lack, J. B., Yassin, A., Sprengelmeyer, Q. D., Johanning, E. J., David, J. R., & Pool, J. E.
580 (2016b). Life history evolution and cellular mechanisms associated with increased
581 size in high-altitude *Drosophila*. *Ecology and evolution*, *6*(16), 5893-5906.
582
583 Lack, J. B., Lange, J. D., Tang, A. D., Corbett-Detig, R. B., & Pool, J. E. (2016c). A
584 Thousand Fly Genomes: An Expanded *Drosophila* Genome Nexus. *Molecular Biology*
585 *and Evolution*, *33*(12), 3308–3313.
586
587 Lange, J. D., & Pool, J. E. (2016). A haplotype method detects diverse scenarios of
588 local adaptation from genomic sequence variation. *Molecular ecology*, *25*(13), 3081-
589 3100.
590
591 Lee, J. R., Urban, S., Garvey, C. F., & Freeman, M. (2001). Regulated Intracellular
592 Ligand Transport and Proteolysis Control EGF Signal Activation in *Drosophila*. *Cell*,
593 *107*(2), 161–171.
594
595 Lee, S. F., Chen, Y., Varan, A. K., Wee, C. W., Rako, L., Axford, J. K., Good, R. T., Blacket,
596 M. J., Reuter, C., Partridge, L., & Hoffmann, A. A. (2011). Molecular Basis of Adaptive

Shift in Body Size in *Drosophila melanogaster*: Functional and Sequence Analyses of the Dca Gene. *Molecular Biology and Evolution*, *28*(8), 2393–2402.

Li, H., & Durbin, R. (2009). Fast and accurate short read alignment with Burrows–Wheeler transform. *Bioinformatics*, *25*(14), 1754–1760.

Liao, B.-Y., Weng, M.-P., & Zhang, J. (2010). Contrasting genetic paths to morphological and physiological evolution. *Proceedings of the National Academy of Sciences*, *107*(16), 7353–7358.

Linnen, C. R., Kingsley, E. P., Jensen, J. D., & Hoekstra, H. E. (2009). On the Origin and Spread of an Adaptive Allele in Deer Mice. *Science*, *325*(5944), 1095–1098.

Liu, Y., Wang, W., Shui, G., & Huang, X. (2014). CDP-Diacylglycerol Synthetase Coordinates Cell Growth and Fat Storage through Phosphatidylinositol Metabolism and the Insulin Pathway. *PLOS Genetics*, *10*(3), e1004172.

Louis, J., David, J., Rouault, J., & Capy, P. (1982). Altitudinal variations of Afro-tropical D. melanogaster populations. *Dros. Inf. Serv*, *58*, 100-101.

Lunter, G., & Goodson, M. (2011). Stampy: A statistical algorithm for sensitive and fast mapping of Illumina sequence reads. *Genome Research*, *21*(6), 936–939.

McCabe, J., & Partridge, L. (1997). An Interaction Between Environmental Temperature and Genetic Variation for Body Size for the Fitness of Adult Female *Drosophila* Melanogaster. *Evolution*, *51*(4), 1164–1174.

McKenna, A., Hanna, M., Banks, E., Sivachenko, A., Cibulskis, K., Kernytsky, A., Garimella, K., Altshuler, D., Gabriel, S., Daly, M., & DePristo, M. A. (2010). The Genome Analysis Toolkit: A MapReduce framework for analyzing next-generation DNA sequencing data. *Genome Research*, *20*(9), 1297–1303.

Miller, C. T., Glazer, A. M., Summers, B. R., Blackman, B. K., Norman, A. R., Shapiro, M. D., Cole, B. L., Peichel, C. L., Schluter, D., & Kingsley, D. M. (2014). Modular Skeletal Evolution in Sticklebacks Is Controlled by Additive and Clustered Quantitative Trait Loci. *Genetics*, *197*(1), 405–420.

Norry, F. M., Bubliy, O. A., & Loeschcke, V. (2001). Developmental Time, Body Size and Wing Loading in Drosophila Buzzatii from Lowland and Highland Populations in Argentina. *Hereditas*, *135*(1), 35–40.

Pennings, P. S., & Hermisson, J. (2006). Soft Sweeps III: The Signature of Positive Selection from Recurrent Mutation. *PLOS Genetics*, *2*(12), e186.

641 Pitchers, W., Pool, J. E., & Dworkin, I. (2013). Altitudinal Clinal Variation in Wing Size
642 and Shape in African *Drosophila melanogaster*: One Cline or Many? *Evolution*, *67*(2),
643 438–452.
644
645 Pool, J. E., Corbett-Detig, R. B., Sugino, R. P., Stevens, K. A., Cardeno, C. M., Crepeau, M.
646 W., Duchen, P., Emerson, J. J., Saelao, P., Begun, D. J., & Langley, C. H. (2012).
647 Population Genomics of Sub-Saharan *Drosophila melanogaster*: African Diversity
648 and Non-African Admixture. *PLOS Genetics*, *8*(12), e1003080.
649
650 Pool, J. E. (2015). The mosaic ancestry of the *Drosophila* genetic reference panel and
651 the D. melanogaster reference genome reveals a network of epistatic fitness
652 interactions. *Molecular biology and evolution*, *32*(12), 3236-3251.
653
654 Pool, J. E. (2016). Genetic mapping by bulk segregant analysis in *Drosophila*:
655 experimental design and simulation-based inference. *Genetics*, *204*(3), 1295-1306.
656
657 Pool, J. E., Braun, D. T., & Lack, J. B. (2017). Parallel evolution of cold tolerance
658 within *Drosophila melanogaster*. *Molecular biology and evolution*, *34*(2), 349-360.
659
660 Pritchard, J. K., & Di Rienzo, A. (2010). Adaptation – not by sweeps alone. *Nature*
661 *Reviews Genetics*, *11*(10), 665–667.
662
663 Prober, D. A., & Edgar, B. A. (2002). Interactions between Ras1, dMyc, and dPI3K
664 signaling in the developing *Drosophila* wing. *Genes & Development*, *16*(17), 2286–
665 2299.
666
667 Reeve, M. W., Fowler, K., & Partridge, L. (2000). Increased body size confers greater
668 fitness at lower experimental temperature in male *Drosophila melanogaster*. *Journal*
669 *of Evolutionary Biology*, *13*(5), 836–844.
670
671 Reiling, J. H., & Hafen, E. (2004). The hypoxia-induced paralogs *Scylla* and *Charybdis*
672 inhibit growth by down-regulating S6K activity upstream of TSC in *Drosophila*.
673 *Genes & Development*, *18*(23), 2879–2892.
674
675 Rockman, M. V. (2012). The QTN Program and the alleles that matter for evolution:
676 All that's gold does not glitter. *Evolution*, *66*(1), 1–17.
677
678 Rutledge, B. J., Zhang, K., Bier, E., Jan, Y. N., & Perrimon, N. (1992). The *Drosophila*
679 *spitz* gene encodes a putative EGF-like growth factor involved in dorsal-ventral axis
680 formation and neurogenesis. *Genes & Development*, *6*(8), 1503–1517.
681
682 Smith, A. V., & Orr-Weaver, T. L. (1991). The regulation of the cell cycle during
683 Drosophila embryogenesis: The transition to polyteny. *Development*, *112*(4), 997–
684 1008.
685

686 Sprengelmeyer, Q. D., Mansourian, S., Lange, J. D., Matute, D. R., Cooper, B. S., Jirle, E.
687 V., Stensmyr, M. C., & Pool, J. E. (2020). Recurrent collection of *Drosophila*
688 *melanogaster* from wild African environments and genomic insights into species
689 history. *Molecular Biology and Evolution 37*(3), 627-638.
690
691 Sprengelmeyer, Q. D., & Pool, J. E. (2021). Ethanol resistance in *Drosophila*
692 *melanogaster* has increased in parallel cold-adapted populations and shows a
693 variable genetic architecture within and between populations. *Ecology and*
694 *Evolution*, Accepted.
695
696 Stalker, H. D., & Carson, H. L. (1948). An Altitudinal Transect of *Drosophila robusta*
697 Sturtevant. *Evolution*, *2*(4), 295–305
698
699 Stephan, W. (2016). Signatures of positive selection: From selective sweeps at
700 individual loci to subtle allele frequency changes in polygenic adaptation. *Molecular*
701 *Ecology*, *25*(1), 79–88.
702
703 Thornton, K. R. (2019). Polygenic Adaptation to an environmental shift: Temporal
704 dynamics of variation under gaussian stabilizing selection and additive effects on a
705 single trait. *Genetics*, *213*(4), 1513–1530.
706
707 Thumm, M., & Kadowaki, T. (2001). The loss of *Drosophila* APG4/AUT2 function
708 modifies the phenotypes of cut and Notch signaling pathway mutants. *Molecular*
709 *Genetics and Genomics*, *266*(4), 657–663.
710
711 Turner, T. L., Stewart, A. D., Fields, A. T., Rice, W. R., & Tarone, A. M. (2011a).
712 Population-Based Resequencing of Experimentally Evolved Populations Reveals the
713 Genetic Basis of Body Size Variation in *Drosophila melanogaster*. *PLOS Genetics*,
714 *7*(3), e1001336.
715
716 van't Hof, A. E., Edmonds, N., Dalíková, M., Marec, F., & Saccheri, I. J. (2011).
717 Industrial melanism in British peppered moths has a singular and recent mutational
718 origin. *Science*, *332*(6032), 958-960.
719
720 Verghese, S., Bedi, S., & Kango-Singh, M. (2012). Hippo signalling controls Dronc
721 activity to regulate organ size in *Drosophila*. *Cell Death & Differentiation*, *19*(10),
722 1664–1676.
723
724 Villano, J. L., & Katz, F. N. (1995). Four-jointed is required for intermediate growth in
725 the proximal-distal axis in *Drosophila*. *Development*, *121*(9), 2767–2777.
726
727 Wang, D., Li, J., Liu, S., Zhou, H., Zhang, L., Shi, W., & Shen, J. (2017). Spalt is
728 functionally conserved in *Locusta* and *Drosophila* to promote wing growth.
729 *Scientific Reports*, *7*(1), 44393.
730

731 Wang, X., Zhang, Y., & Blair, S. S. (2019). Fat-regulated adaptor protein Dlish binds
732 the growth suppressor Expanded and controls its stability and ubiquitination.
733 *Proceedings of the National Academy of Sciences*, *116*(4), 1319–1324.
734
735 Yeaman, S., & Whitlock, M. C. (2011). The genetic architecture of adaptation under
736 migration–selection balance. *Evolution: International Journal of Organic*
737 *Evolution*, *65*(7), 1897-1911.
738
739 Zinke, I., Kirchner, C., Chao, L. C., Tetzlaff, M. T., & Pankratz, M. J. (1999). Suppression
740 of food intake and growth by amino acids in *Drosophila*: The role of pumpless, a fat
741 body expressed gene with homology to vertebrate glycine cleavage system.
742 *Development*, *126*(23), 5275–5284.
743
744
745
746
747

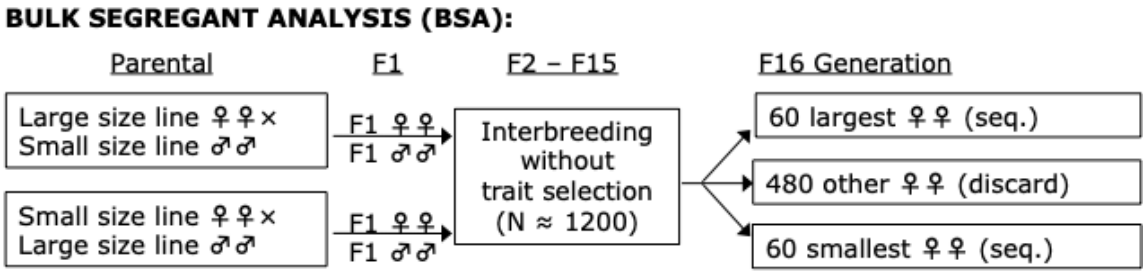

Figure 1. The bulk QTL mapping experimental design is illustrated. As further described in the Materials and Methods, F1 offspring of reciprocal crosses were allowed to interbreed in a relatively large population without selection until the F15 generation, at which point 600 females were sorted to obtain the top and bottom 10% for a size trait for sequencing. This design allows a large number of unique recombination events to take place, which should improve mapping performance.

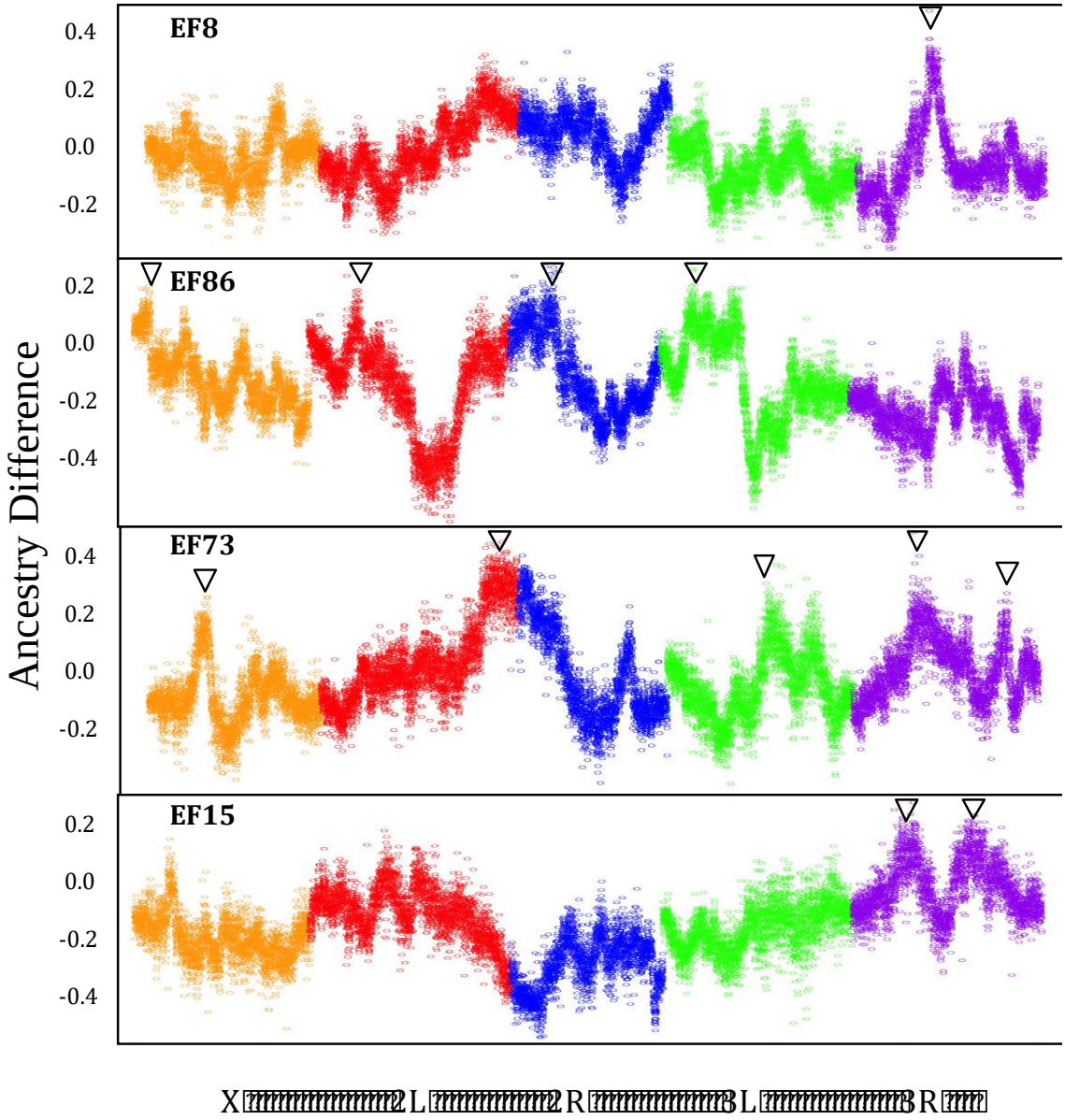

Figure 2. Significant QTL peaks for four Ethiopia/Zambia thorax length crosses. A point for each ~8 kb window corresponds to the average difference in ancestry from the larger parental strain between the large and small F16 pools (y-axis). Significant primary or secondary QTL peaks are denoted with an arrow. The significance threshold for primary peaks is approximately 0.17.

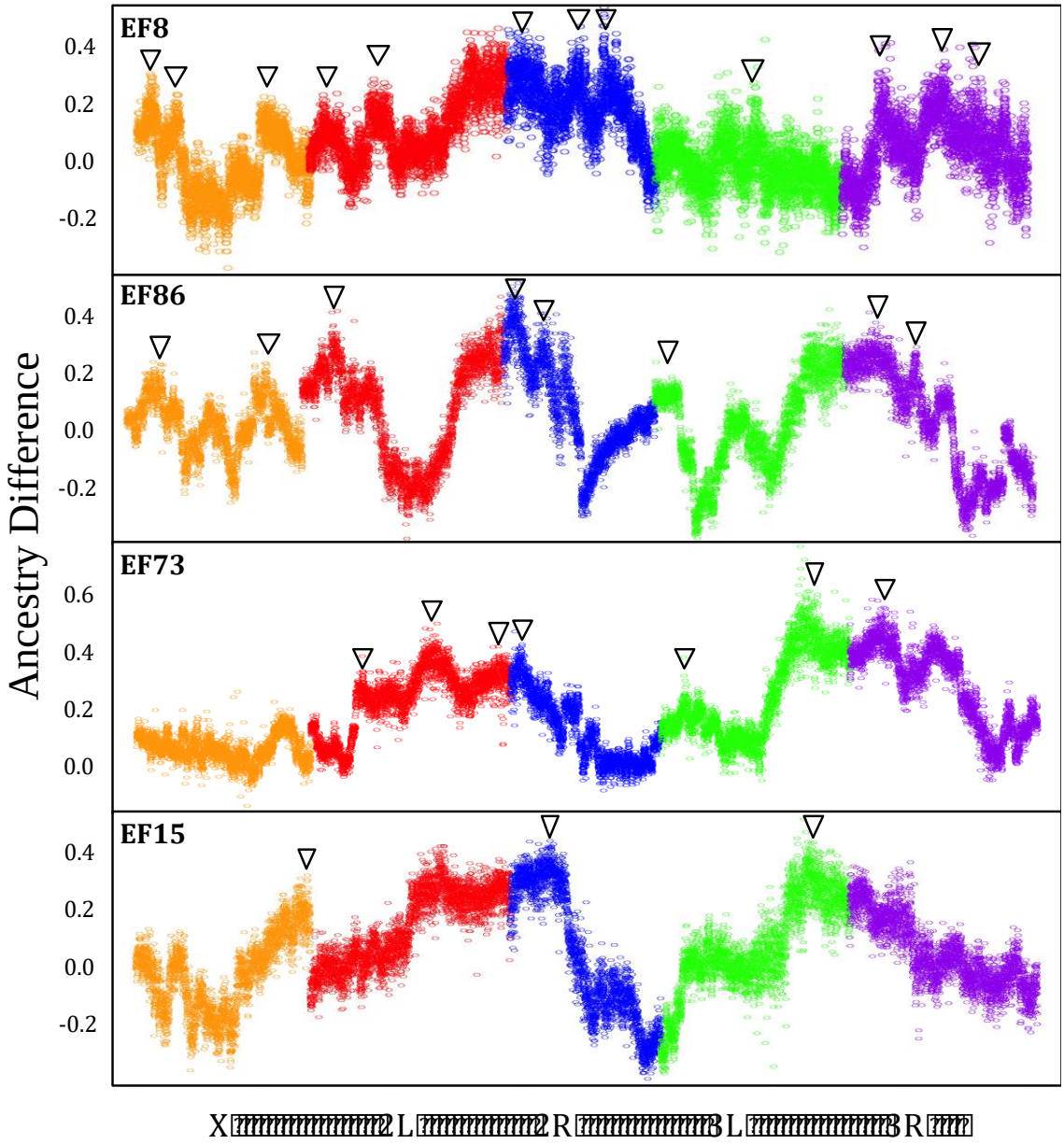

767
768 **Figure 3**. Significant QTL peaks for four Ethiopia/Zambia wing length crosses. A
769 point for each ~8 kb window corresponds to the average difference in ancestry from
770 the larger parental strain between the large and small F16 pools (y-axis). Significant
771 primary or secondary QTL peaks are denoted with an arrow. The significance
772 threshold for primary peaks is approximately 0.17.

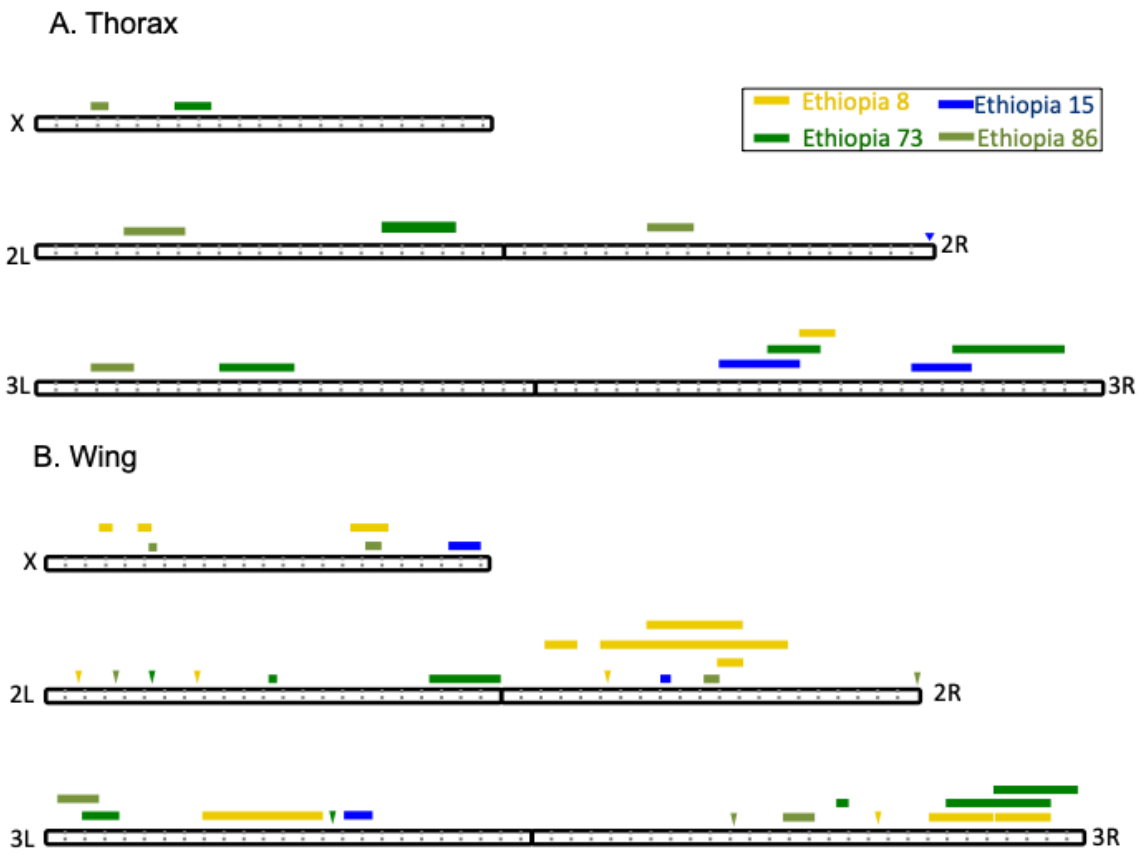

Figure 4. The locations of significant QTLs on the five euchromatic chromosome arms of *D. melanogaster*. The colors indicate for four Ethiopia strains used in mapping crosses for **A**) thorax length and **B**) wing length. The width of each box indicates the 90% C.I. of each QTL. Intervals that are less than 10 kb in width are marked with triangles. Dotted gray lines indicate Mb increments.

786

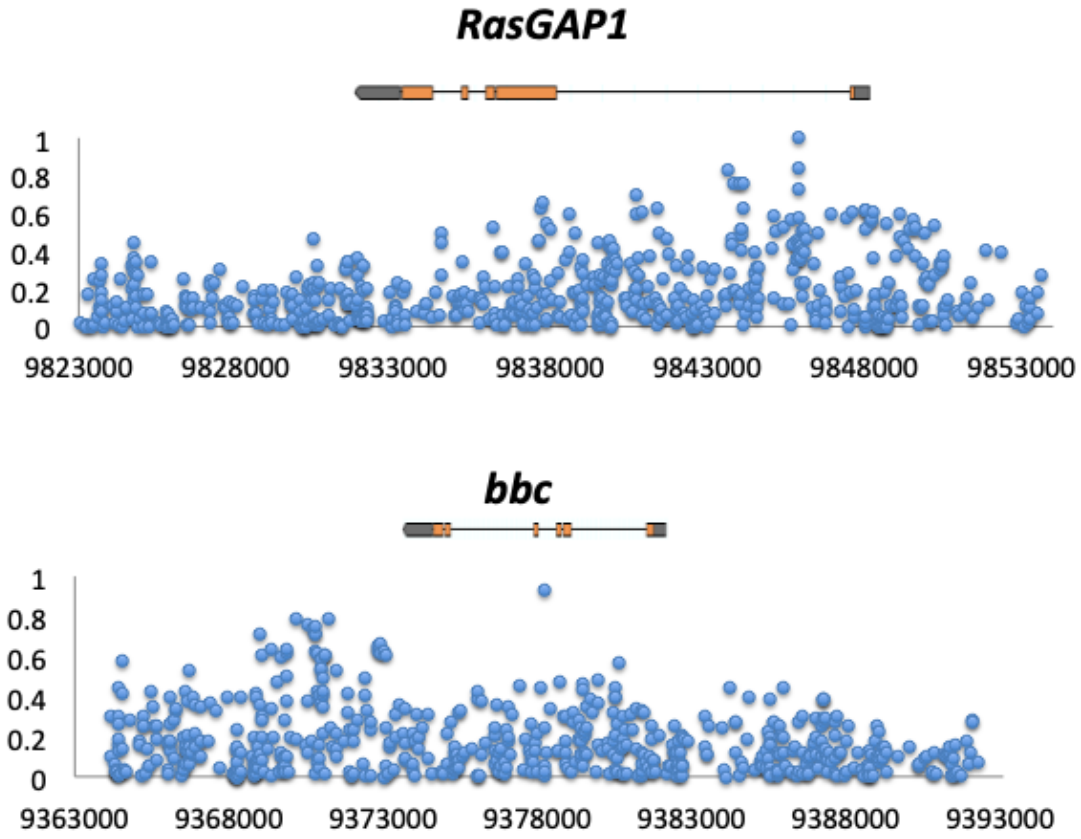

787
788

789 **Figure 5**. At two candidate genes identified for thorax length evolution (*bbc* and
790 *RasGAP1*), small numbers of SNPs show the highest F_{ST} values between Ethiopia and
791 Zambia. Depicted above is the gene transcript, while the x-axis indicates bp position
792 along the relevant chromosome arm (release 5).

793
794
795

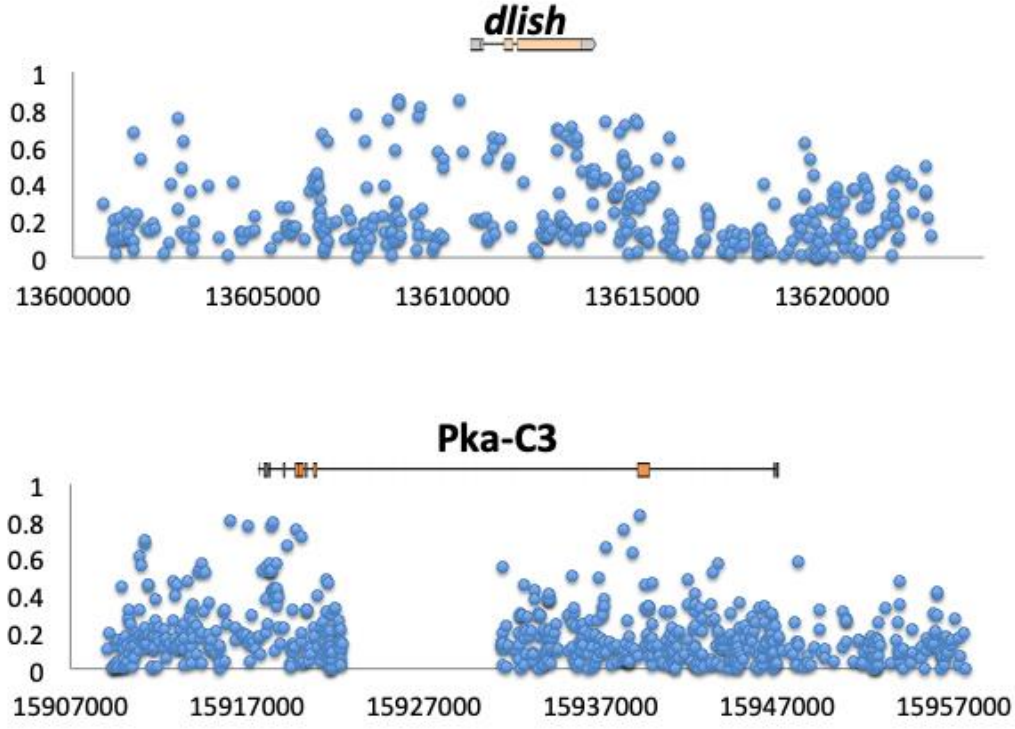

796

797 **Figure 6**. Peaks of SNP F_{ST} center on two candidate genes identified for wing size
798 evolution (*dlish* and *Pka-C3*), showing elevated genetic differentiation between
799 Ethiopia and Zambia at these genes. Depicted above is the gene transcript, while the
800 x-axis indicates bp position along the relevant chromosome arm (release 5).
801

802

803

804

805

806

807

808

809

Trait	Avg. QTLs per Cross	Pairwise QTL Overlap	Avg. Effect Size
Ethanol Resistance	8	35%	14%
Thorax Length	3	0%	15%
Wing Length	8.25	36%	17%
Stripe Width	3	8%	19%
Background Color	5.67	18%	19%

Table 1. The results of bulk QTL mapping experiments for five different traits. All mapping used the same experimental design described in the Materials and Methods, aside from minor variation in the number of generations of interbreeding (15-20). Both the pigmentation stripe and pigmentation background data is from Bastide et al. (2016), while the ethanol results are from Sprengelmeyer & Pool (2021). Listed are the number of significant QTLs for each mapping population, the proportion of QTLs that overlap between parallel crosses from the same two populations, and the average QTL effect size across all mapping crosses.

Table S3. Locations and properties of significant QTLs identified in wing size mapping by SIBSA

ResistantPar	ChromArm	PeakWinStar	PeakWinStop	PeakHeight	PeakType	PValue
EF15N	X	20904702	20909740	0.23377199	primary	0.00046667
EF15N	2R	8188459	8195793	0.32972987	primary	0
EF15N	3L	15922228	15938382	0.31607979	primary	0
EF86N	X	5463507	5470072	0.24273786	primary	0.00015
EF86N	X	16305411	16313884	0.24218895	primary	0.00012
EF86N	2L	3387229	3391271	0.35169247	primary	0
EF86N	2R	3179097	3193215	0.45434109	primary_clust	0
EF86N	2R	10474932	10485101	0.30755203	secondary_cl	0
EF86N	3L	455784	463634	0.20524852	primary	0.00326667
EF86N	3R	10363556	10371495	0.32910121	primary_clust	0
EF86N	3R	13848437	13855026	0.2943865	secondary_cl	0.02797203
EF8N	X	3066352	3071088	0.22110349	primary_clust	0.0023
EF8N	X	6248759	6256499	0.19644059	secondary_cl	0
EF8N	X	16535731	16544112	0.17713694	primary	0.04775
EF8N	2L	1772611	1777569	0.18756562	secondary_cl	0.03076923
EF8N	2L	7658982	7663712	0.20783816	secondary_cl	0.03846154
EF8N	2R	5112157	5123897	0.31261537	secondary_cl	0.00384615
EF8N	2R	12022195	12027092	0.29982165	secondary_cl	0.00384615
EF8N	2R	14672013	14680160	0.34755072	primary_clust	0
EF8N	3L	10882366	10886176	0.17690647	primary	0.039
EF8N	3R	17528562	17539172	0.25420175	primary_clust	1.00E-04
EF8N	3R	21094931	21103488	0.22944425	secondary_cl	0.03082192
EF8N	3R	25121535	25127327	0.20182695	secondary_cl	0
EF73N	2L	5448027	5454090	0.30895823	secondary_cl	0.016
EF73N	2L	11507264	11514787	0.39403868	primary_clust	0
EF73N	2L	19759251	19766791	0.34496582	secondary_cl	0.04
EF73N	2R	3510107	3522552	0.3804457	secondary_cl	0
EF73N	2R	11238857	11249335	0.23019477	secondary_cl	0.004
EF73N	3L	2551676	2558009	0.22631683	primary	0.0014
EF73N	3L	14511249	14517354	0.55499451	primary_clust	0
EF73N	3R	15679500	15694164	0.4333253	secondary_cl	0.02608696
EF73N	3R	24354594	24365687	0.18778311	primary	0.01586
EF73N	3R	26932176	26936632	0.1955858	primary	0.0113

M.

	Effect Size	Effect Size 90% CI		QTL Location 90% CI	
MatchingSim	PropVarExpla	PropVar5th	PropVar95th	LeftBoundPo	RightBoundPos
387	0.1643822	0.09719545	0.22122642	20525343	21934418
257	0.23961623	0.17818535	0.28169584	8076976	8414273
293	0.23173917	0.17295992	0.27589939	15063943	16462676
325	0.18528431	0.12832031	0.24011869	5382824	5594427
345	0.18764033	0.12210868	0.23766864	16161667	16428059
291	0.25073404	0.20135708	0.29853666	3213559	3536859
347	0.12134529	0.03983746	0.21869686	21999618	3378149
347	0.14873684	0.07934142	0.2079711	10254368	11002593
369	0.1511218	0.07708819	0.21149543	251545	2704736
1272	0.17532648	0.10591747	0.23975909	10363556	10371495
1272	0.1177756	0.05497032	0.19143452	12826840	14108781
1225	0.13904385	0.07151736	0.20256078	2714235	3263115
1225	0.1258279	0.06010287	0.18568678	4848276	6266234
389	0.13038966	0.06095335	0.19344116	15586962	17404497
112	0.14905406	0.07028348	0.22020014	1772611	1777569
112	0.15624434	0.07839896	0.22328034	7658982	7663712
112	0.23227995	0.11632569	0.28879125	5112157	5123897
112	0.12936744	0.01133562	0.24881377	7224772	12031486
112	0.24083484	0.1029423	0.30856012	5061973	14686338
392	0.12427832	0.06285144	0.19199097	8010928	14179576
175	0.13581961	0.07889708	0.18736355	17528562	17539172
175	0.07348323	0.04240819	0.13085448	20308960	23144977
175	0.07340696	0.04538591	0.12810356	23498145	26177221
116	0.21467493	0.13484872	0.28164547	5374526	5527676
116	0.25998313	0.14903659	0.33650601	11291188	11934541
116	0.0584702	0.00841488	0.19966073	19648840	2325076
116	0.22065396	0.06152621	0.29973585	2352478	3762273
116	0.13173246	0.04990698	0.2038664	11037010	12168889
349	0.16722651	0.09463971	0.23237536	1786941	3799405
620	0.27037423	0.21804692	0.32827304	14511249	14517354
620	0.19954508	0.1429355	0.26060988	15392115	16010049
379	0.14124829	0.07070685	0.19557706	21293120	26152658
405	0.14464796	0.07699061	0.2047368	23319999	27758980